**NUCLEAR DATA AND MEASUREMENTS SERIES**

**ANL/NDM-137**

# Neutron Scattering and Models: Silver

by

A.B. Smith

July 1996

**ARGONNE NATIONAL LABORATORY,**
**ARGONNE, ILLINOIS 60439, U.S.A.**

# NUCLEAR DATA AND MEASUREMENTS SERIES

ANL/NDM-137

NEUTRON SCATTERING AND MODELS:-SILVER

A. B. Smith
July, 1996

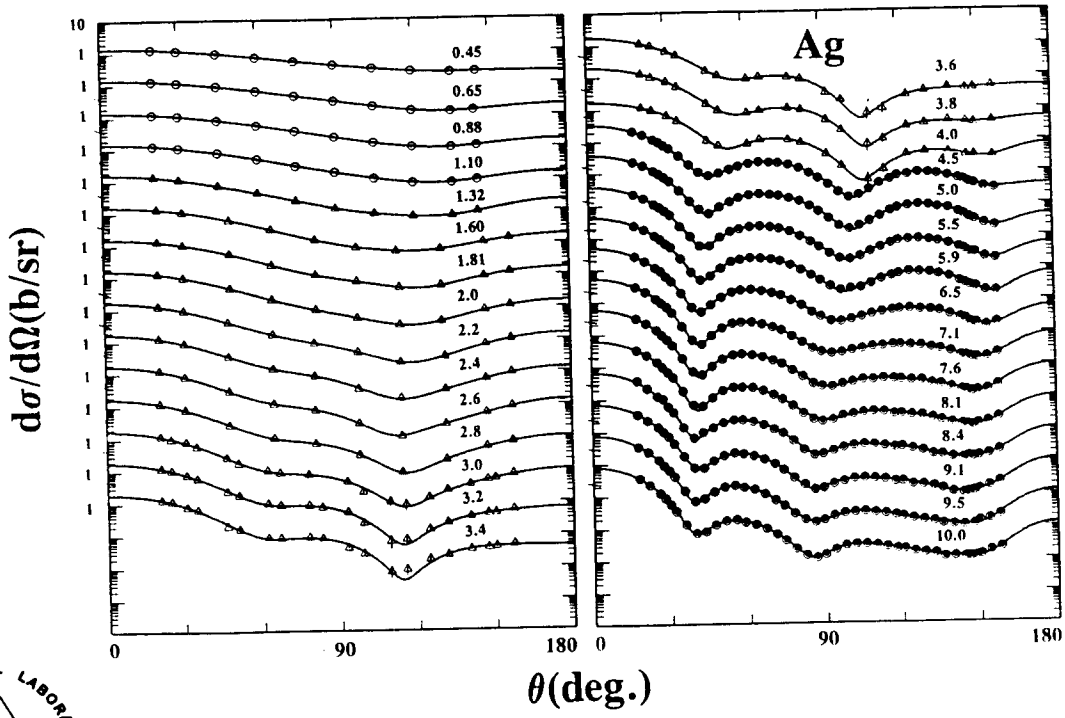


**ARGONNE NATIONAL LABORATORY, ARGONNE, ILLINOIS**
Operated by THE UNIVERSITY OF CHICAGO
for the U. S. DEPARTMENT OF ENERGY
under Contract W-31-109-Eng-38

## Argonne National Laboratory

Argonne National Laboratory, with facilities in the states of Illinois and Idaho, is owned by the United States Government, and operated by the University of Chicago under provisions of a contract with the Department of Energy.

---

## Disclaimer



---

Reproduced from the best available copy.

Available to DOE and DOE contractors from the Office of Scientific and Technical Information, P. O. Box 62, Oak Ridge, TN 37831; prices available from (423) 576-8401.

Available to the public from the National Technical Information Service, U. S. Department of Commerce, 5285 Port Royal Road, Springfield, VA 22161.

ANL/NDM-137

# NEUTRON SCATTERING AND MODELS:- SILVER*

by

A. B. Smith

Argonne National Laboratory
Argonne, Illinois
and
The University of Arizona
Tucson, Arizona

July, 1996

---

Keywords:
Measured $d\sigma/d\Omega_{el}$ and $d\sigma/d\Omega_{inel}$ (1.5 → 10 MeV) for neutrons incident on elemental silver. Comprehensive optical and coupled-channels model interpretations.

---

* This work supported by the United States Department of Energy under contract W-31-109-Eng-38, and by the Nuclear and Energy Engineering Program, College of Engineering and Mines, University of Arizona.

## PUBLICATIONS IN THE ANL/NDM SERIES

A listing of recent issues in this series is given below. Issues and/or titles prior to ANL/NDM-120 can be obtained from the National Technical Information Service, U. S. Department of Commerce, 5285 Port Royal Road, Springfield, VA 22161, or by contacting the author of this report at the following address:-

Technology Development Division
Argonne National Laboratory
9700 South Cass Avenue
Argonne, IL 60439
USA

A. B. SMITH, P. T. GUENTHER, J. F. WHALEN, AND S. CHIBA
*Fast-neutron Total and Scattering Cross Sections of $^{58}Ni$ and Nuclear Models*
ANL/NDM-120, July 1991

S. CHIBA AND D. L. SMITH
*A Suggested Procedure for Resolving an Anomaly in Least-squares Data Analysis Known as "Peelle's Pertinent Puzzle" and the General Implications for Nuclear Data Evaluation*
ANL/NDM-121, September 1991

D. L. SMITH AND DOMINIQUE FEAUTRIER
*Development and Testing of a Deuterium Gas Target Assembly for Neutron Production Via the H-2(D,N)HE-3 Reaction at a Low-energy Accelerator Facility*
ANL/NDM-122, March 1992

D. L. SMITH AND E. T. CHENG
*A Review of Nuclear Data Needs and Their Status for Fusion Reactor Technology with some Suggestions on a Strategy to Satisfy the Requirements*
ANL/NDM-123, September 1991

J. W. MEADOWS
*The Thick-Target $^{9}Be(d,n)$ Neutron Spectra for Deuteron Energies Between 2.6 and 7.0-MeV*
ANL/NDM-124, November 1991

A. B. SMITH AND P. T. GUENTHER
*Fast-Neutron Scattering Near Shell Closures:- Scandium*
ANL/NDM-125, August 1992

A. B. SMITH, J. W. MEADOWS AND R. J. HOWERTON
*A Basic Evaluated Neutronic Data File for Elemental Scandium*
ANL/NDM-126, November 1992

A. B. SMITH AND P. T. GUENTHER
*Fast-Neutron Interaction With Vibrational Cadmium Nuclei*
ANL/NDM-127, November 1992

D. L. SMITH
*A Least-Squares Computational "Tool Kit"*
ANL/NDM-128, April 1993

JOSEPH McCABE, A. B. SMITH AND J. W. MEADOWS
*Evaluated Nuclear Data Files for the Naturally-Occurring Isotopes of Cadmium*
ANL/NDM-129, June 1993

A. B. SMITH AND P. T. GUENTHER
*Fast-Neutron Interaction with the Fission Product* $^{109}Rh$
ANL/NDM-130, September 1993

A. B. SMITH AND P. T. GUENTHER
*Fast-Neutron Scattering from Vibrational Palladium Nuclei*
ANL/NDM-131, October 1993

A. B. SMITH
*Neutron Interaction with Doubly-Magic* $^{40}Ca$
ANL/NDM-132, December 1993

A. B. SMITH
*Neutron Scattering at Z = 50:- Tin*
ANL/NDM-133, September 1994

A. B. SMITH, S. CHIBA AND J. W. MEADOWS
*An Evaluated Neutronic File for Elemental Zirconium*
ANL/NDM-134, September 1994

A. B. SMITH
*Neutron Scattering from Elemental Uranium and Thorium*
ANL/NDM-135, February 1995

A. B. SMITH
*Neutron Scattering and Models:- Iron*
ANL/NDM-136, August 1995

TABLE OF CONTENTS

ANL/NDM-137

# NEUTRON SCATTERING AND MODELS:- SILVER

by

A. B. Smith

Argonne National Laboratory
Argonne, Illinois
and
The University of Arizona
Tucson, Arizona

## ABSTRACT

Differential neutron elastic-scattering cross sections of elemental silver were measured from 1.5 → 10 MeV at ≈ 100 keV intervals up to 3 MeV, at ≈ 200 keV intervals from 3 → 4 MeV, and at ≈ 500 keV intervals above 4 MeV. At ≤ 4 MeV the angular range of the measurements was ≈ $20^0$ → $160^o$ with 10 measured values below 3 MeV and 20 from 3 → 4 MeV at each incident energy. Above 4 MeV ≥ 40 scattering angles were used distributed between ≈ $17^o$ and $160^o$. All of the measured elastic distributions included some contributions due to inelastic scattering. Below 4 MeV the measurements determined cross sections for ten inelastically-scattered neutron groups corresponding to observed excitations of 328 ± 13, 419 ± 50, 748 ± 25, 908 ± 26, 1150 ± 38, 1286 ± 25, 1507 ± 20, 1623 ± 30, 1835 ± 20 and 1944 ± 26 keV. All of these inelastic groups probably were composites of contributions from the two isotopes $^{107}$Ag and $^{109}$Ag. The experimental results were interpreted in terms of the spherical optical model and of rotational and vibrational coupled-channels models, and physical implications are discussed. In particular, the neutron-scattering results are consistent with a ground-state rotational band with a quadrupole deformation $\beta_2$ = 0.20 ± ≈10% for both of the naturally-occurring silver isotopes.

## 1. Introduction

Elemental silver consists of approximately equal parts of the two transitional nuclei $^{107}$Ag (51.8%) and $^{109}$Ag (48.2%). Both of these isotopes have essentially the same low-energy structure characterized by a $1/2^-$ ground state (g.s.), followed by a $(7/2^+, 9/2^+)$ doublet at ≈ 110 keV, and a $(3/2^-, 5/2^-)$ doublet at ≈ 360 keV [NDS]. Heavy-ion studies attribute this structure to a quasi-particle configuration coupled to a slightly deformed (e.g., $\beta_2 \approx 0.12$) even-even prolate rotational core [Ric+77, Pop+79], with a variable moment of inertia and including coriolis perturbations. This model leads to a negative-parity rotational band based upon the $1/2^-$ g.s., then a positive-parity $\Delta I = 1$ band based upon the $9/2^+$ level at about 125 keV, and accounts for the "anomalous" yrast $7/2^+$ state. Alternate interpretations based upon triaxial models give similar results but involve larger quadrupole deformations (e.g., $\beta_2 \approx 0.2$) [Kel+85, Kal+79, Paa73]. At higher excitation energies high-spin rotational bands in the silver isotopes have been suggested [Jer+94, Jer+94A, Kel+85, Kal+79] with very large, or "super", deformations similar to those reported in the neighboring palladium isotopes [Mac+88, Jer+93, Ric+77, SR76]. It was suggested that such strong "super" deformations are characteristic of the A ≈ 100 region. Neutron scattering at ≤ 10 MeV is sensitive to the collective properties of low-energy excitations well below the coulomb barrier. Unfortunately, there is very little experimental knowledge of neutron scattering from silver above ≈ 1.5 MeV. A number of global spherical optical-statistical models have been reported in the literature [You86] but give quite different results in the MeV region when applied to silver, and of course none of them address the collective aspects of the interaction. Studies of proton scattering from $^{107}$Ag suggest a collective vibrational interaction [For+67], and an attempt has been made to model neutron total cross sections of silver using a vibrational mechanism [Lag80]. However, the vibrational mechanism may be inconsistent with some aspects of the heavy-ion studies. The isotopes of silver lie near the peak of the fission-product yield curve thus their neutronic properties are of interest from the point of view of the fission-reactor fuel cycle. Since there are low-lying excited states in such isotopes with small spin differences, the inelastic-scattering cross sections should be large at the low energies of fission-reactor interest.

The above considerations motivated the present work directed toward the experimental definition of neutron scattering from silver in the low-MeV range and its interpretation. Section 2 very briefly outlines the experimental methods, Section 3 presents the experimental results, Section 4 summarizes extensive

model interpretations using spherical-optical and coupled-channels (rotational and vibrational) models, and Section 5 discusses and summarizes the results. Early low-energy portions of this work were described in the Laboratory report of ref. [SG82]. The experimental data reported herein has been transmitted to the National Nuclear Data Center, Brookhaven National Laboratory.

## 2. Experimental Methods

All of the measurements were made using the fast-neutron time-of-flight method [CL55] and the Argonne ten-angle detection system. This method and apparatus have been amply described elsewhere [Smi+92] and therefore only details specific to the present measurements will be outlined here. The measurement sample was a cylinder of high-purity metallic elemental silver 2 cm in diameter and 2 cm long. Below 4 MeV the $^{7}Li(p,n)^{7}Be$ neutron-source reaction was employed with incident-neutron energy spreads of 50 to 100 keV [Dro87]. Above 4 MeV the $D(d,n)^{3}He$ reaction was used as a source with energy spreads of ≈ 300 keV at 4 MeV, decreasing to ≈ 100 keV at 10 MeV [Dro87]. The mean neutron energy was determined to within ≈ 10 keV by control of the incident ion beam. The neutron sources were pulsed at a 2 MHz repetition rate with a burst duration of ≈ 1 nsec. Ten collimated scattered-neutron flight paths ≈ 5 m long were arranged about the sample with liquid-scintillation detectors placed at their ends. Below 4 MeV the silver cross sections were determined relative to the carbon total cross section using the method described in ref. [SGM82], and at higher energies relative to the H(n,n) scattering standard [CSL83]. All of the silver cross sections were corrected for beam-attenuation, multiple-event and angular-resolution effects using Monte-Carlo techniques [Smi91].

## 3. Experimental Results

### 3.1. Elastic Scattering

The elastic-scattering measurements were made in two steps. The first dealt with the lower incident energies of 1.5 to 4 MeV. In this set the measurements were made at incident-energy intervals of ≈ 100 keV up to 3 MeV, and at ≈ 200 keV intervals from 3 to 4 MeV. The experimental angular range extended from ≈ $20^{o}$ to $160^{o}$ in ten increments below 3 MeV and in twenty increments from 3 to 4 MeV. The incident energy spreads and the scattered-neutron resolutions were arranged so that the "elastic" scattering included contributions due to the inelastic excitation of the yrast $7/2^{+}$ and $9/2^{+}$ levels (i.e., included inelastic contributions resulting from excitation energies of <≈ 135 keV). The estimated uncertainties associated with the differential

values ranged from ≈ 5% to larger amounts at the minima of the distributions. These lower-energy results are illustrated in Fig. 3.1.1.

From 4.5 to 10 MeV the elastic-scattering results were obtained at ≈ 0.5 MeV incident-neutron intervals, with ≥ 40 differential values measured at each incident energy distributed between ≈ $17^{o}$ and $160^{o}$. The incident-neutron energy spread, the scattered-neutron resolution and the summations of the experimental time spectra were adjusted so that the measured "elastic" scattering included inelastic contributions due to excitation of the yrast $7/2^{+}$, $9/2^{+}$, $3/2^{-}$ and $5/2^{-}$ levels (i.e., a scattered-neutron resolution of ≈ 450 keV). The model interpretations described below specifically account for these inelastic perturbations (and the similar but smaller effects associated with the above lower-energy data). Contributions due to the excitation of the $7/2^{+}$ and $9/2^{+}$ levels were quite small, but those due to the $3/2^{-}$ and $5/2^{-}$ levels were appreciable. The estimated uncertainties attributed to the higher-energy results ranged from 3%-4% to larger values at the minima of the distributions, including contributions from; statistics, angular uncertainties, normalization and the correction procedures. The higher-energy elastic scattering results are summarized in Fig. 3.1.2.

There is very little silver neutron elastic-scattering information reported in the literature comparable with the present measurements [Buc+66, Bec+66, MS62]. The ≤ 4 MeV $^{107}$Ag elastic-scattering results of ref. [Smi+79] are consistent with the present elemental elastic-scattering results.

## 3.2. Inelastic Scattering

At incident energies of ≤ 4 MeV inelastic-scattering measurements were made concurrently with the elastic-scattering studies. Given the incident energy spreads, the relatively broad scattered-neutron resolutions and the the complexity of the level structures of the contributing $^{107}$Ag and $^{109}$Ag isotopes, it was not generally possible to resolve neutron scattering from any explicit level in either isotope. Rather, ten scattered-neutron groups corresponding to apparent excitations of 328±13, 419±50, 748±25, 908±26, 1150±38, 1286±25, 1507±20, 1623±30, 1835±20 and 1944±26 keV were observed. The cited energy uncertainties are rms deviations of a number of measurements from their means and do not necessarily imply the distribution of individual excitation energies. In addition, a few high-resolution measurements provided quite small cross sections for the excitation of levels at ≈ 110 keV. Most of these observed neutron groups can be reasonably associated with the reported

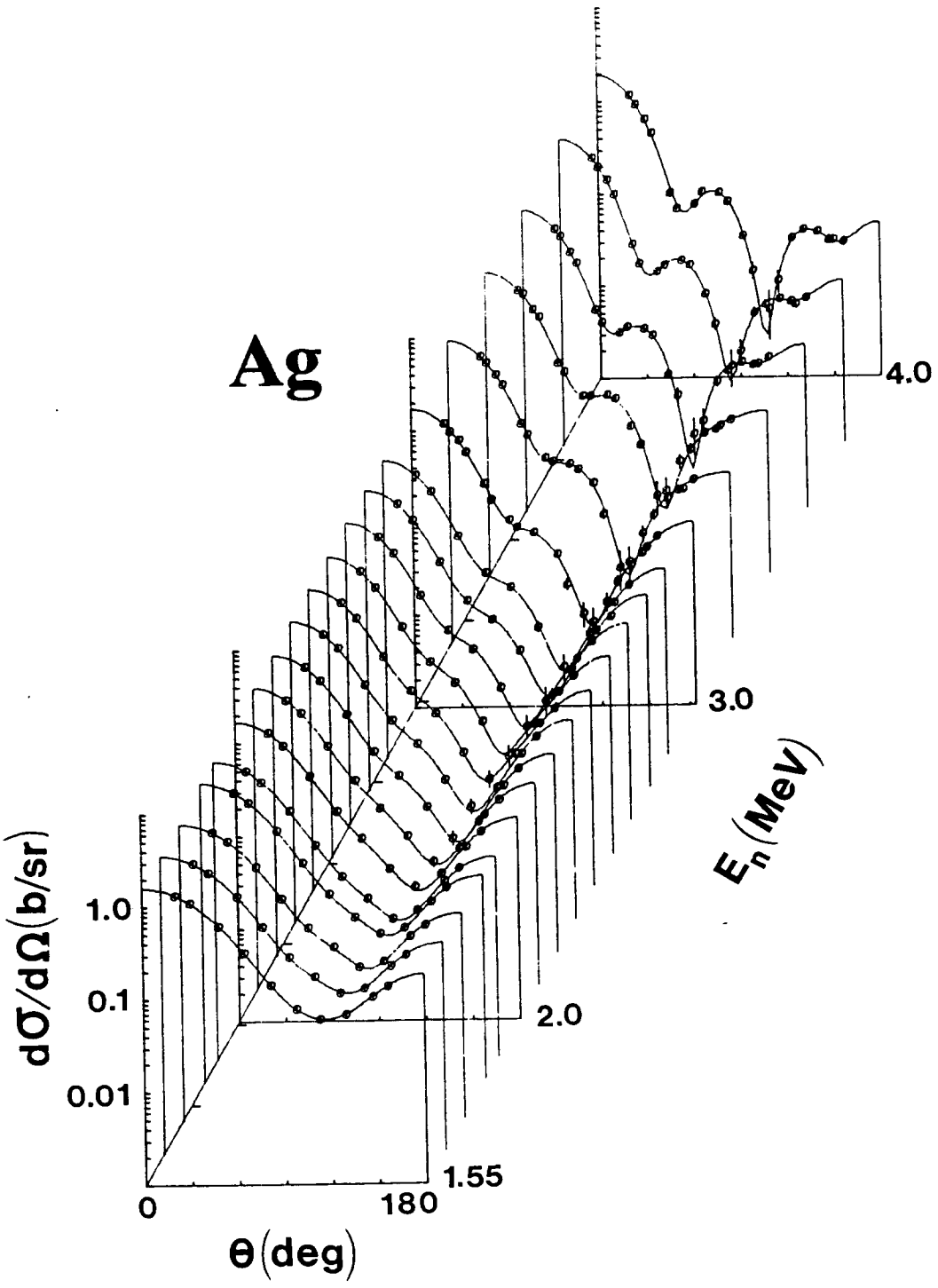


Fig. 3.1.1. Differential elastic-scattering cross sections of elemental silver over the incident energy range ≈ 1.5 to 4 MeV. Experimental values are indicated by symbols and the results of Legendre-polynomial fitting with curves. Throughout this paper differential data are presented in the laboratory coordinate system.

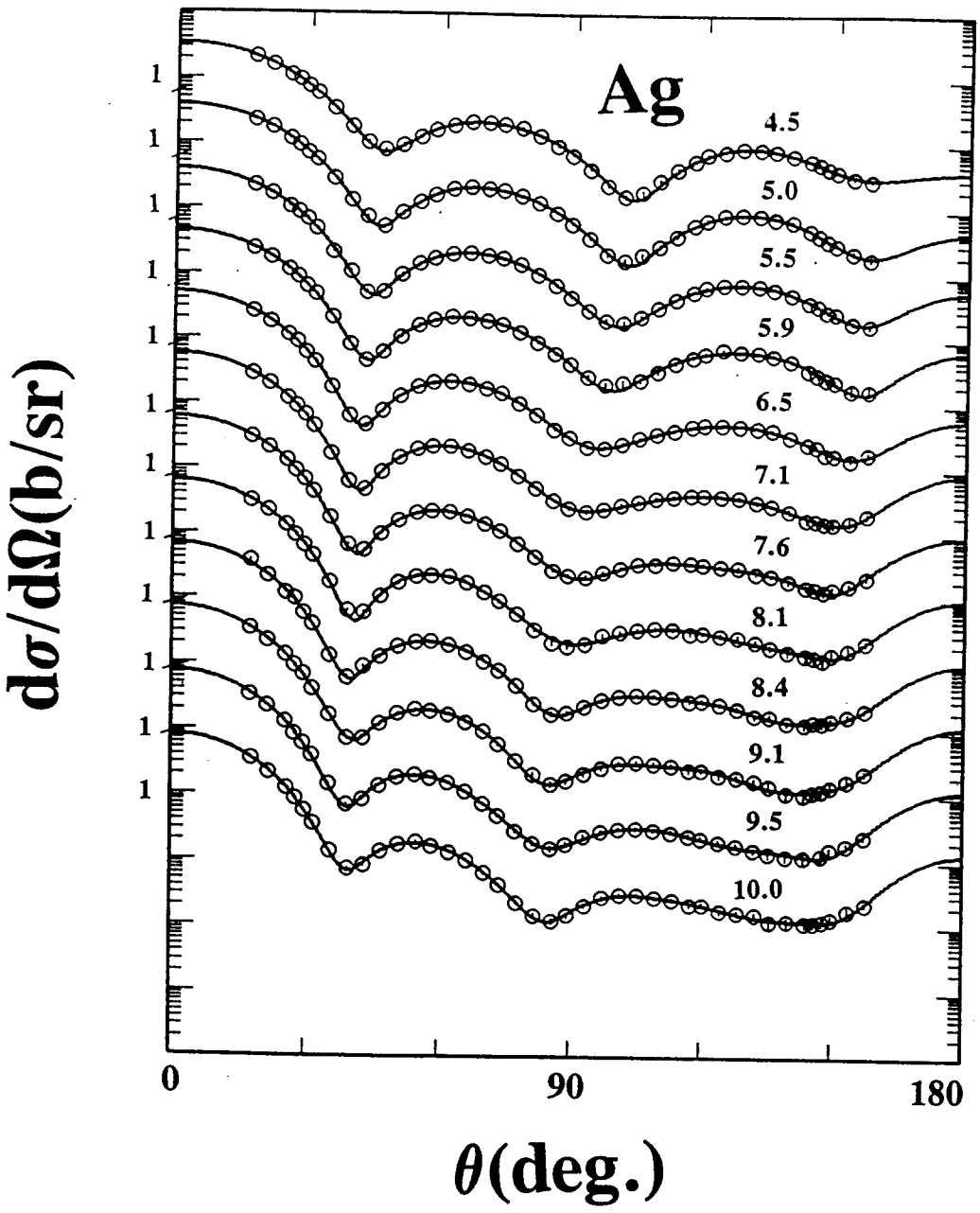


Fig. 3.1.2. Higher-energy differential elastic-scattering results for elemental silver, as described in the text. Experimental values are indicated by symbols, and the results of Legendre-polynomial fitting by curves. Approximate incident energies are numerically cited.

levels in $^{107}Ag$ and $^{109}Ag$ as given in Table 1 of ref. [SG82]. The observed inelastically-scattered neutrons were approximately isotropically distributed. The corresponding angle-integrated cross sections were determined by fitting low-order Legendre-polynomial expansions to the experimental values. The angle-integrated results were corrected for perturbations due to the second neutron group from the $^{7}Li(p,n)^{7}Be$ source reaction where appropriate. These corrections were large in some cases (e.g., near excitations of ≈ 400 kev), and increased the uncertainties in the angle-integrated results. Corrections to the differential angular distributions were not attempted as at some excitation and incident energies the forward-angle perturbation from the source reaction was the dominant contribution to the observed neutron scattering. The uncertainties associated with the angle-integrated results are quite large (e.g., 10% to 30%), primarily due to correction procedures and statistics. The angle-integrated inelastic-scattering results are summarized in Fig. 3.2.1. They are reasonably consistent with the $^{107}Ag$ inelastic-scattering results of ref. [Smi+79].

## 4. Model Interpretations

The model interpretations had the objectives of; i) providing a phenomenological vehicle for describing, interpolating and extrapolating the experimental results (particularly for applied purposes), ii) contributing to regional (or even global) representations of neutron scattering, and iii) correlating the experimental observations with physical concepts, particularly the collective nature of the silver isotopes at low energies.

### 4.1. Data Base

The interpretations placed primary emphasis upon elastic-scattering data, essentially all of which comes from the Argonne program. From 0.3 to 1.5 MeV the results of Vonach and Smith [VS65] were averaged over ≈ 200 keV intervals to form the lower-energy portion of the data base. From 1.5 to 4 MeV the present work was used, supplemented with the $^{107}Ag$ results of Smith et al. [Smi+79]. Again, the measured values were averaged over ≈ 200 keV in order to smooth any residual fluctuations and to reduce the size of the data base to more manageable proportions. The elemental and isotopic data were treated independently. From 4 to 10 MeV reliance was placed entirely on the present results. The literature appears to contain very little silver elastic-scattering data at energies above ≈ 1.5 MeV and none above 10 MeV. Above ≈ 1.1 MeV the elastic-scattering data all contains some inelastic-scattering perturbations which were explicitly dealt with in the interpretations as described below. The elemental elastic-scattering data base used in the

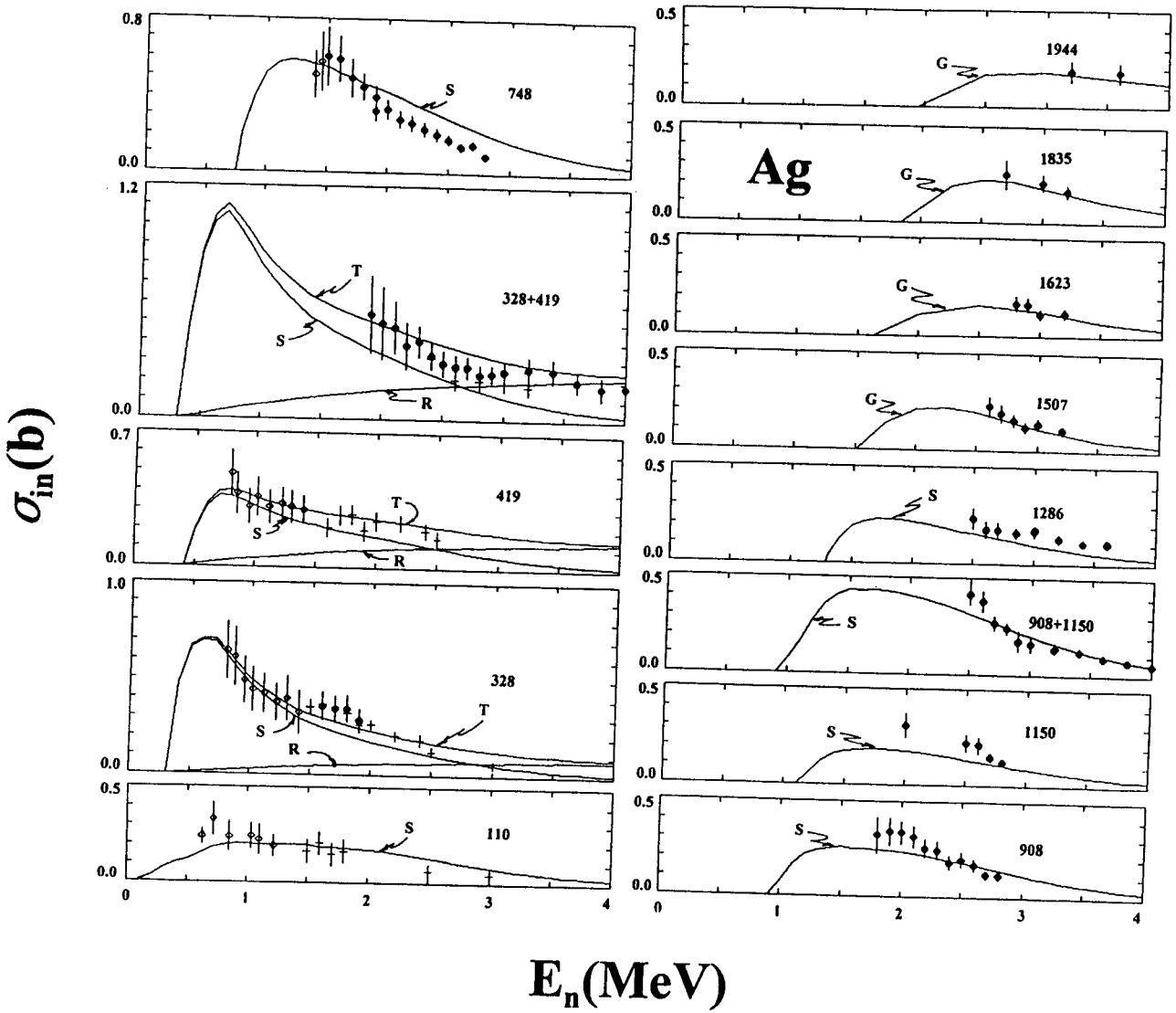


Fig. 3.2.1. Angle-integrated inelastic-scattering cross sections of elemental silver as defined in the text. Symbols indicate experimental values where; i) solid circles are from the present work, ii) open circles from ref. [VS65] and iii) crosses from the $^{107}$Ag results of ref. [Smi+79]. Curves indicate; "S" SOM results, "R" ROTM direct-reaction results, "T" the total inelastic cross sections combining CN and direct results, and "G" are simple eyeguides. Observed excitation energies are numerically noted in keV (in some cases sums of contributions are given).

fitting is illustrated in Fig. 4.1.1. Secondary attention was given to the elemental neutron total cross sections taken from refs. [PW83, MW66, CB67 and FG71], and averaged over ≈ 100 keV to smooth fluctuations and to reduce the number of experimental values. Comparisons were made with the present inelastic-scattering results and those of refs. [VS65 and Smi+79]. Comparisons were also made with strength functions taken from ref. [MDH81].

## 4.2. Potential Forms

Throughout the interpretations the real potential was assumed to have the Saxon-Woods (SW) form, the surface-absorption imaginary potential the SW-derivative form, and the spin-orbit potential (assumed real and non-deformed) the Thomas form [Hod71]. Throughout the calculations the parameters of the spin-orbit potential given by Walter and Guss [WG86] were used. Where volume-absorption was considered it was assumed to have the SW form with the geometric parameters of the real potential.

## 4.3. Spherical Optical Model (SOM)

The derivation of a model from experimental data, or the description of experimental results with a model, is governed by the validity of the physical assumptions underlying the model. In the context of the present neutron scattering from elemental silver the SOM is not a particularly attractive assumption as it does not account for the direct inelastic-scattering processes that are very significant in the observed "elastic" and inelastic scattering above several MeV. The unsuitability of the SOM is reflected in unfortunate results from the fitting at some energies and in a difference between model parameters deduced from high- and low-energy portions of the data base. Therefore, considerable subjective judgment was used in the SOM derivation and it is reasonable to expect model results which are not entirely consistent with the experimental values. Despite these shortcomings the SOM for silver is of some interest in the provision of data for applications, and can be used as a basis for DWBA calculations in more basic studies. For these reasons a SOM was derived.

The SOM was primarily obtained by explicit chi-square fitting of the elastic-scattering data base. The calculational tool was a version of the spherical optical-model code ABAREX [Mol82] that explicitly treated both the $^{107}$Ag and $^{109}$Ag isotopes of the element. Compound-nucleus processes were calculated using the Hauser-Feshbach formula [HF52] as modified by Moldauer to account for resonance width fluctuation and correlation effects [Mol80]. The calculations employed twelve discrete excitations for $^{107}$Ag and thirteen for $^{109}$Ag with the energies, spins and parities given in the Nuclear Data Sheets [NDS]. These discrete excitations extended to energies of approximately one MeV.

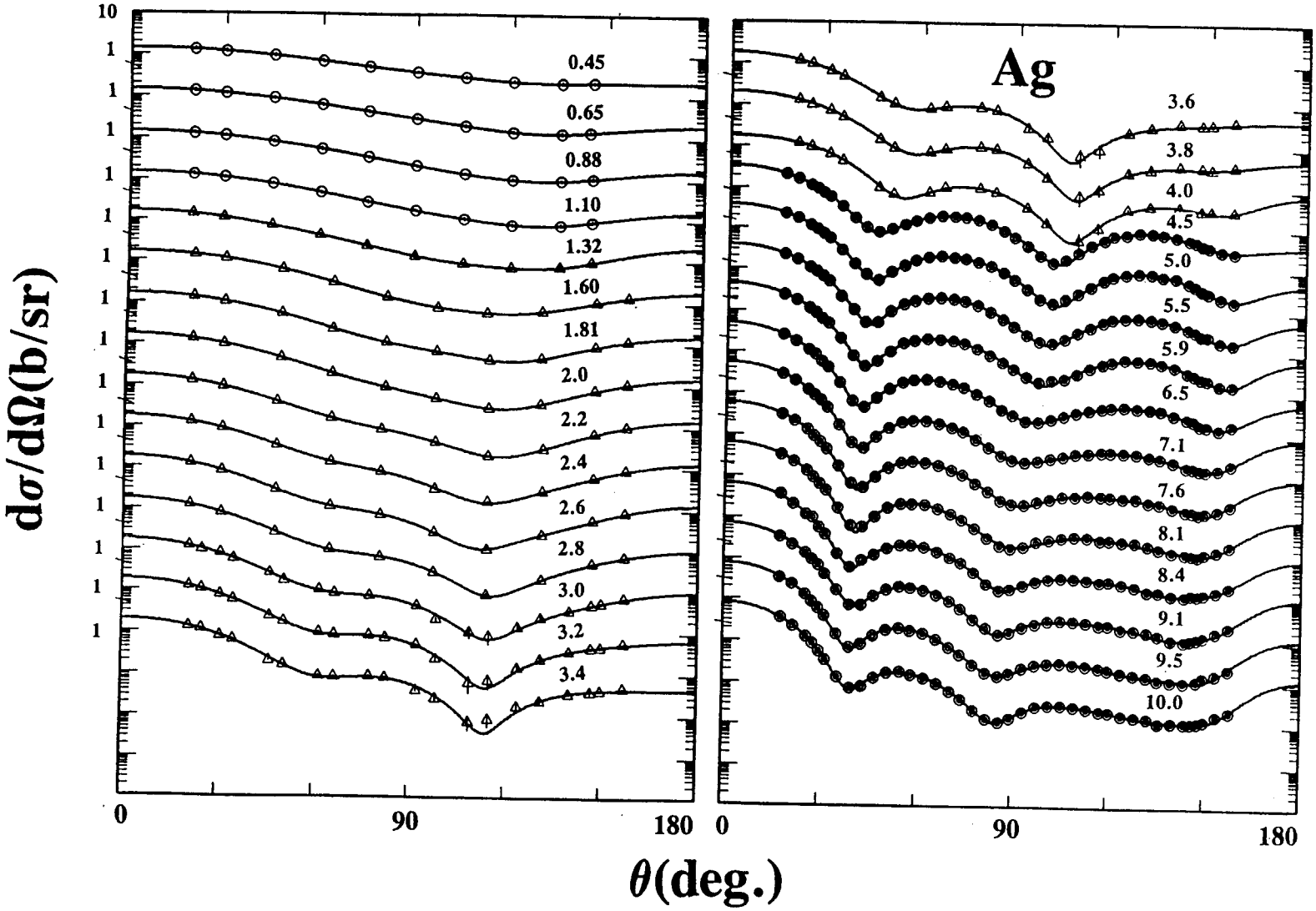


Fig. 4.1.1. The elemental elastic-scattering data used in the fitting. Symbols indicate experimental results where; simple circles note elastic scattering, triangles elastic scattering plus contributions from the first two inelastic neutron-groups, and concentric circles elastic scattering plus contributions from the first four inelastic-neutron groups. Approximate incident energies are numerically noted.

Higher-energy excitations were calculated using the statistical representation of Gilbert and Cameron [GC65]. At incident energies > 1.1 MeV the calculations combined the elastic and inelastic contributions in a manner consistent with the above-cited resolutions of the experimental data used in the data base (i.e., combining the elastic contribution with the first two or four inelastic components before evaluating chi-square). The fitting procedures followed the five-step regime long used at this laboratory [Smi+92]; i) first fixing the real-potential diffuseness, $a_v$, using six-parameter fitting varying real and imaginary potential strengths, radii and diffusenesses, ii) then five-parameter fitting to fix the real-potential radius, $r_v$, iii) four-parameter fitting to fix the imaginary-potential radius, $r_w$, iv) three-parameter fitting to obtain the imaginary-potential diffuseness, $a_w$, and finally v) two-parameter fitting to determine real, $J_v$, and imaginary, $J_w$, potential strengths (herein potential strengths $J_i$ are presented as volume-integrals-per-nucleon and radii $r_i$ in the reduced form where the full radius $R_i = r_i \cdot A^{1/3}$, unless otherwise explicitly stated). This fitting regime is sensitive to the well-know correlations of real-potential magnitude and radius and imaginary-potential magnitude and diffuseness. However, these correlations are mitigated by the large sample, and the procedure avoids an initial fixation upon any particular region of the parameter space. Due to the multi-isotopic nature of the elemental sample, comprehensive compound-nucleus treatment, the non-zero g.s. spin of the target isotopes and the extensive fitting, the calculations were tedious.

Following the above fitting regime, the SOM parameters of Table 4.3.1 were obtained. (Throughout this work model-parameters are given to sufficient precisions to permit accurate reproduction of the calculated results. These precisions do not necessarily imply accuracies which are generally approximately three significant figures.) These SOM parameters provide the description of the elemental elastic-scattering data base illustrated in Fig. 4.3.1. A similar description of the $^{107}$Ag elastic-scattering below 4 MeV [Smi+79] was obtained. At lower energies, the SOM represents the compound-nucleus inelastic scattering as illustrated in Fig. 3.2.1. As the energy increases the direct reactions become appreciable and the SOM less suitable. The measured elemental total cross sections are compared with the calculated values in Fig. 4.3.2, and comparisons of calculated strength functions with those deduced from measurements is given in Table 4.3.2. The experimental data of the present work does not extend beyond 10 MeV and into a region where volume absorption could be a potential concern [Rap+79], thus it is not surprising that the introduction of volume absorption into the SOM fitting procedure

did not significantly improve the description of the measured values.

## 4.4. The Coupled-Channels Model (CCM)

Comprehensive multi-isotopic fitting using the coupled-channels model in the manner employed for the SOM, is forbiddingly time consuming. Therefore, some simplifying assumptions were made. It was assumed that the target was an even nucleus with mass A = 108, the mean of the two elemental isotopes, and a g.s. $J^{\pi} = 0^{+}$. Both of the naturally-occurring silver isotopes have $1/2^{-}$ ground states. The first two excited states in either isotope are of positive parity, have relatively large spin, and are weakly excited by neutron scattering (see Fig. 3.2.1) thus they were ignored. The third and fourth excited states are $3/2^{-}$ and $5/2^{-}$ levels in each isotope and are quite strongly excited by inelastic neutron scattering, and the excitations persist to relatively high energies where CN contributions must be small. Thus, it appears that the excitation of these two states has a significant collective direction-reaction component. It was assumed that this can be represented by the excitation of a $2^{+}$ level at 369 keV in the pseudo A = 108 target. The energy is the weighted mean of the isotopic values. Higher-lying discrete levels were assumed to be those of $^{109}$Ag up to excitations of ≈ 1.0 MeV. This is a rather crude approximation but the corresponding excited levels of $^{107}$Ag are very similar, and discrete CN excitations in the relatively narrow energy band of ≈ 0.5 to 1.0 MeV have a rather modest influence on the model determination. Higher-lying excitations were statistically represented using the formalism of Gilbert and Cameron [GC65] as in the SOM derivation. Thus the CCM deals with a simple even-even nucleus with a g.s. of $0^{+}$, a yrast collective $2^{+}$ excited state at 369 keV, and with CN excitations extending to higher energies. Implicit in the above is the assumption that the collective nature of neutron interaction with the two isotopes $^{107,109}$Ag is essentially the same. This is a reasonable in view of the similarity of the spectroscopy of all the odd silver isotopes [NDS] and coulomb-excitation results of ref. [Rob+70]. The model is an example of "the fictitious even-nucleus approximation" of Lagrange [Lag80]. Heavy-ion studies [Ric+77, Pop+79, Kel+85] suggest that the collective motion of the g.s. band should be rotational. On the other hand, proton-scattering studies suggest a vibrational interaction [For+67], and a neutron study has used a vibrational assumption [Lag80] with some success. Here attention is given to both the rotational model (ROTM) and an alternative vibrational model (VIBM).

Table 4.3.1. SOM parameters. Strengths ($J_i$) are given in terms of volume-integals-per-nucleon (MeV-fm$^3$) (except for the spin-orbit potential where strength is given in MeV), energy (E) is in MeV and geometrical dimensions are in fermis.*

Real Potential

$J_v = 439.8 - 2.8694 \cdot E$

$r_v = 1.2710$

$a_v = 0.6029$

Imaginary Potential

$J_w = 112.1 - 11.95 \cdot E + 0.57594 \cdot E^2$

$r_w = 1.3215$

$a_w = 0.4570$

Spin-Orbit Potential

$Vso = 6.027 - 0.015 \cdot E$

$r_{so} = 1.103$

$a_{so} = 0.56$

* Radii are expressed in the form $R_i = r_i \cdot A^{1/3}$, where "A" is the target mass.

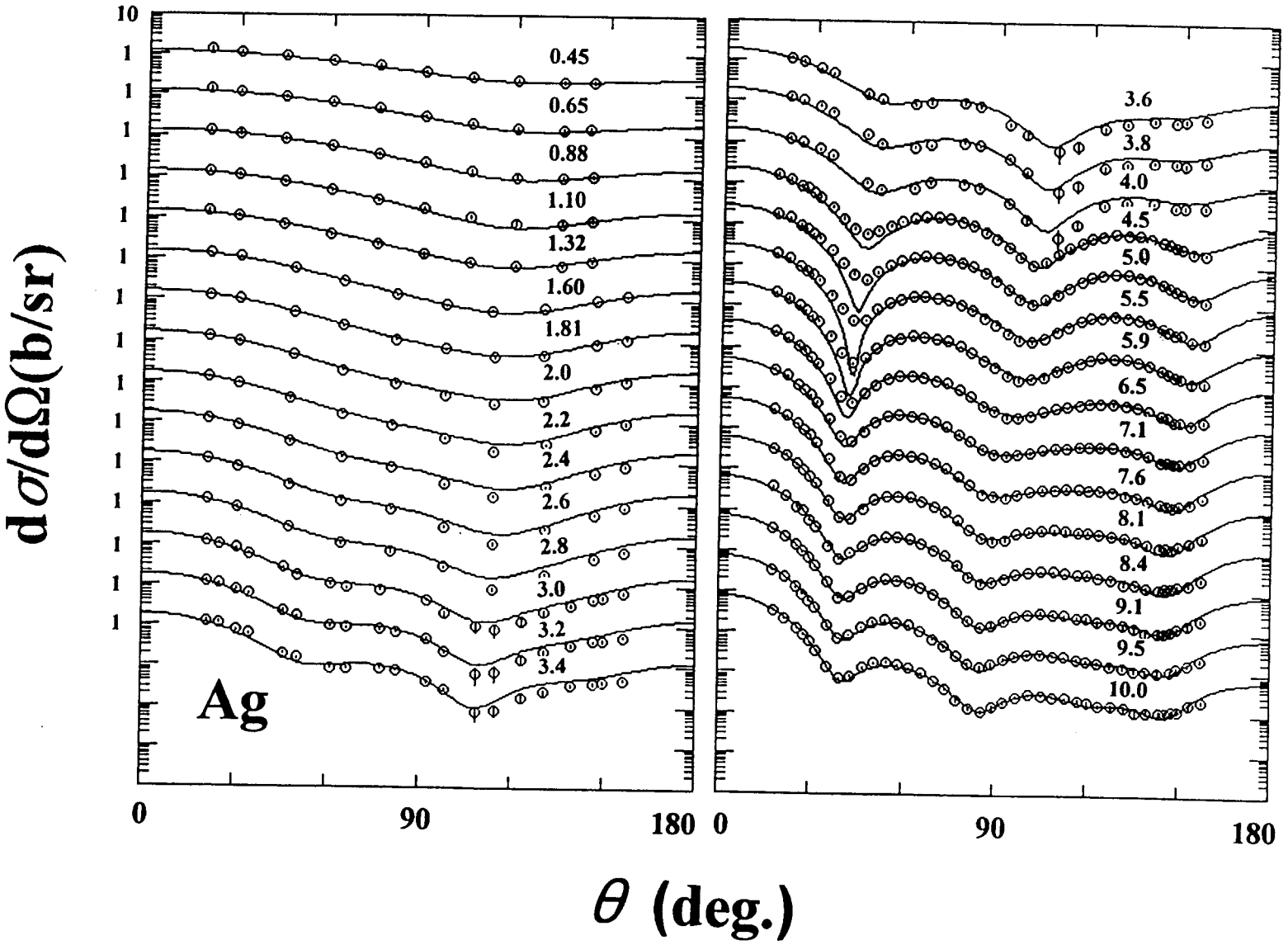


Fig. 4.3.1. Comparison of the elemental elastic-scattering data base with the results of the SOM calculations. Experimental values are indicated by symbols and curves denote the results of SOM calculations. Approximate incident energies are numerically noted.

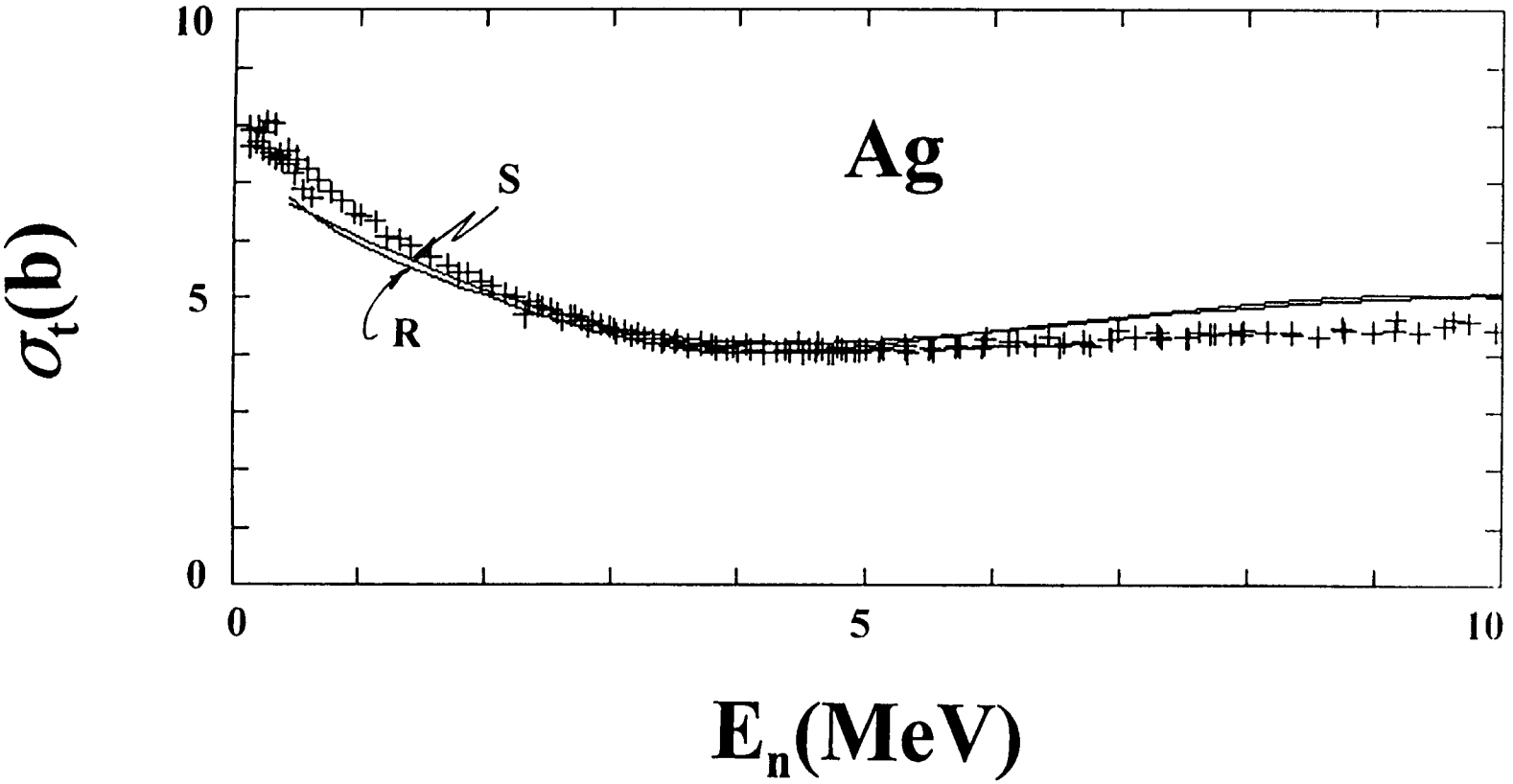


Fig. 4.3.2. Elemental silver total cross sections. Averages of the experimental values are indicated by symbols, referenced as defined in the text, and curves the results of SOM ("S") and ROTM ("R") calculations.

Table 4.3.2. Measured and calculated strength functions of $^{107}Ag$ in units of $10^{-4}$.

| Source | $S_o$ | $S_1$ |
|---|---|---|
| Exp. [MDH81] | 0.38±0.07 | 3.8±0.6 |
| SOM | 1.09 | 4.7 |
| ROTM | 0.79 | 2.7 |
| VIBM | 0.55 | 2.5 |

The CCM rotational (ROTM) fitting followed the five-step procedure outlined above for the SOM, using the coupled-channels code ECIS95 [Ray95]. CN processes were treated in the same manner as for the SOM. Again, elastic and inelastic components were combined in the calculations to be consistent with the experimental resolutions. The entire ROTM fitting procedure was repeated for $\beta_2$ values of 0.00, 0.10, 0.15, 0.20 and 0.25. From comparisons of the calculated and measured elastic-scattering, total cross sections and inelastic-scattering cross sections (as discussed in Section 5, below) it was evident that $\beta_2$ is $\approx$ 0.2 $\pm$ $\approx$10%. The resulting ROTM potential parameters are given in Table 4.4.1. The calculated and measured elastic-scattering cross sections are compared in Fig. 4.4.1, and similar comparisons of total cross sections are given in Fig. 4.3.2. ROTM strength functions are given in Table 4.3.2, and the calculate direct inelastic scattering is shown in Fig. 3.2.1. An analogous approach was used in determining the parameters of the VIBR model. It was assumed that the elemental results could again be reasonably approximated using the pseudo-even nucleus of mass A = 108 as for the ROTM case. A simple one-phonon vibrator was assumed and $\beta_2$ limited to the 0.20 value of the ROTM. The resulting potential parameters are given in Table 4.4.2. The results of the VIBR calculations are compared with the measured elastic scattering in Fig. 4.4.2. Calculated VIBM strength functions are given in Table 4.3.2. Generally, in the context of the neutron interaction to 10 MeV, the ROTM and VIBM give essentially the same results.

## 5. Discussion and Summary

The SOM only crudely approximates the neutron interaction with silver. In some energy regions (e.g., about $\approx$ 5.5 MeV) the calculated elastic scattering differs from the measured values by more than an order of magnitude (see Fig. 4.3.1). At other energies the description is reasonably good. Furthermore, the fitting procedure behaved erratically yielding considerably different parameters at low and high energies where the direct inelastic component in the observed elastic distributions is different. The ROTM and VIBM calculations with $\beta_2$ = 0.2 quite nicely describe the elastic-scattering data as illustrated in Figs. 4.4.1 and 4.4.2. There are only minor differences between measured a calculated values at the highest energies near 10 MeV. Fitting with values of $\beta_2$ less than 0.2 led to results progressively approaching those of the less suitable SOM as the $\beta_2$ magnitude was reduced.

The SOM led to the inelastic-scattering cross sections shown in Fig. 3.2.1. They are in reasonable agreement with the observed values where the latter are primarily due to CN

Table 4.4.1. ROTM parameters obtained with the rotational assumption and a $\beta_2 = 0.20$, as described in the text. The nomenclature is the same as in Table 4.3.1.

Real Potential

$$J_v = 477.0 - 4.6143 \cdot E$$

$$r_v = 1.2945$$

$$a_v = 0.6690$$

Imaginary Potential

$$J_w = 82.45 - 6.6418 \cdot E + 0.3926 \cdot E^2$$

$$r_w = 1.4594 - 0.01264 \cdot E$$

$$a_w = 0.09277 + 0.04824 \cdot E$$

Spin-Orbit Potential (same as in Table 4.3.1)

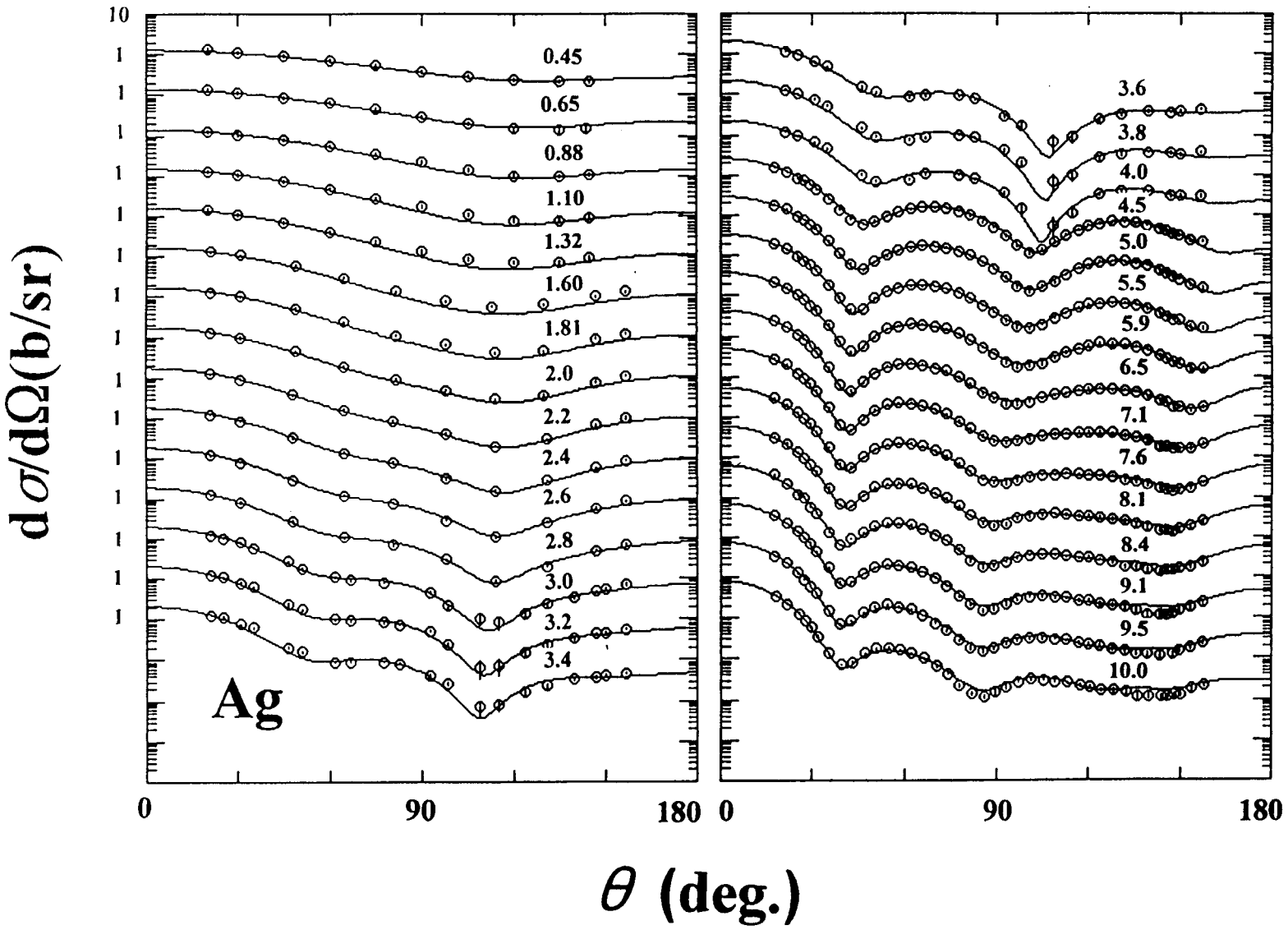


Fig. 4.4.1. Comparison of the elemental elastic-scattering data base with the results of ROTM calculations. The nomenclature is identical to that of Fig. 4.3.1.

Table 4.4.2. VIBM parameters obtained with the vibrational assumption and a $\beta_2 = 0.20$, as described in the text. The nomenclature is the same as in Table 4.3.1.

Real Potential

$$J_v = 458.8 - 2.966 \cdot E$$

$$r_v = 1.3059$$

$$a_v = 0.6938$$

Imaginary Potential

$$J_w = 101.8 - 14.227 \cdot E + 1.0061 \cdot E^2$$

$$r_w = 1.4868 - 0.01511 \cdot E$$

$$a_w = 0.10311 + 0.085882 \cdot E - 0.0042018 \cdot E^2$$

Spin-Orbit Potential (same as in Table 4.3.1)

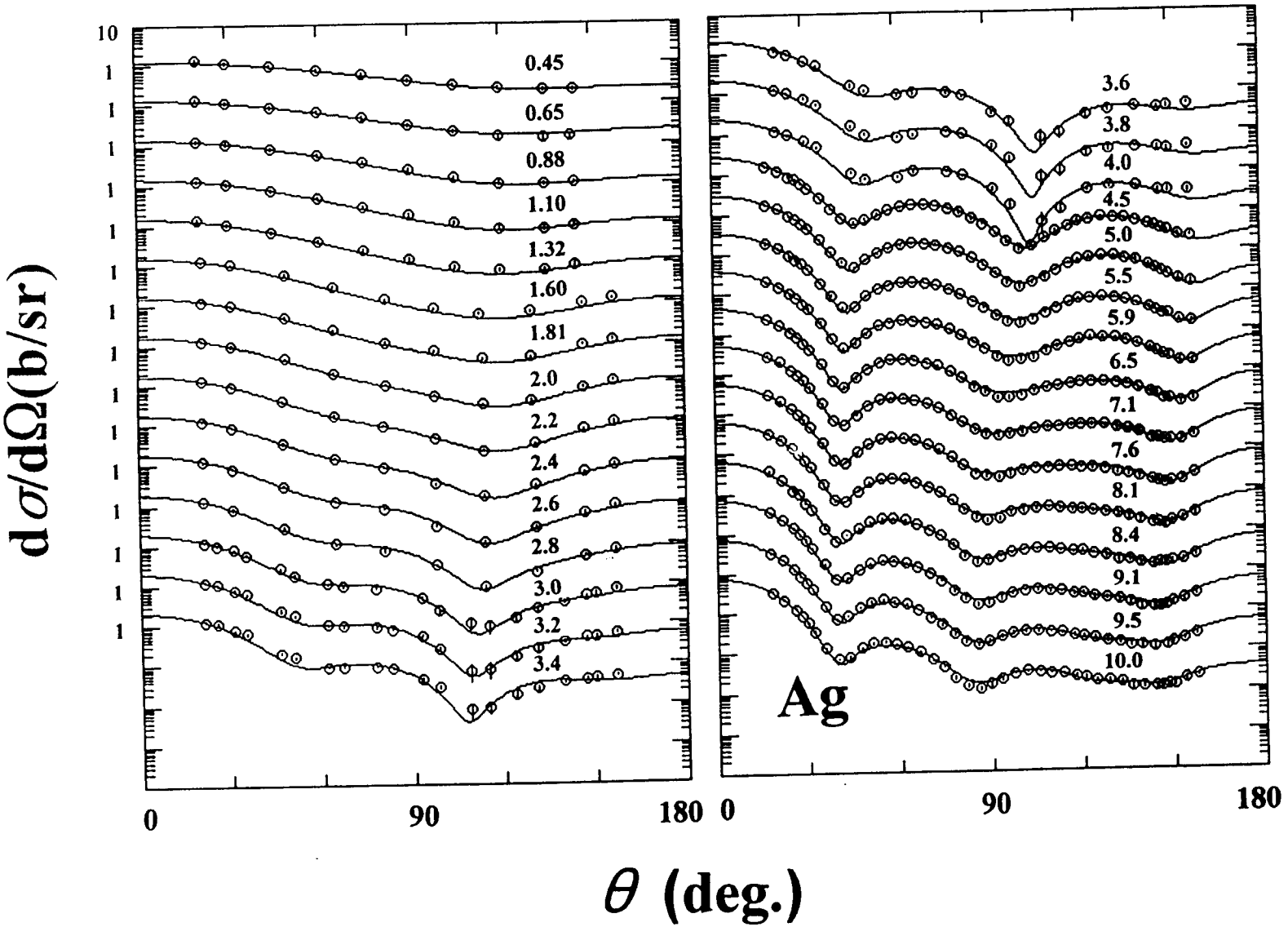


Fig. 4.4.2. Comparison of the elemental elastic-scattering data base with the results of VIBM calculations. The nomenclature is identical to that of Fig. 4.3.1.

processes. Essentially the same CN results were obtained with the SOM, ROTM and VIBM as differences due to the use of transmission coefficients calculated with spherical or deformed potentials are small. However, the ROTM also provides an estimate of the direct inelastic excitation of the 328 ($3/2^-$) and 419 ($5/2^-$) keV levels which is in reasonable agreement with the measured values, (as illustrated in Fig. 3.2.1 where the calculated $2^+$ results are apportioned by 2J+1). Results obtained fitting with $\beta_2$ = 0.15, = 0.10 and (of course) = 0.0 gave progressively less suitable descriptions of the measured inelastic scattering. Results obtained fitting with $\beta_2$ = 0.25 also provide a reasonable description of the the observed elastic and inelastic scattering, but not of the total cross section, as noted below. The quadrupole deformation, $\beta_2$, of $^{107}$Ag and $^{109}$Ag has been reported from coulomb-excitations studies [Rob+70] with results that are quite consistent with the $\beta_2$ = 0.20 of the present work. The average of values from neighboring palladium and cadmium targets is ≈ 0.208, very close to that obtained in this work. A somewhat larger value results from averages of $\beta_2$ of $^{106}$Pd and $^{108}$Pd which may form the collective cores of the present neutron scattering. Proton-scattering studies, assuming vibrational collective processes, resulted in a $\beta_2$ for $^{107}$Ag approximately 10% larger than the present value [For+67] (i.e., consistent with the present result within the respective uncertainties). Some of the interpretations of spectroscopic heavy-ion studies based upon the assumption of a soft prolate rotor coupled with a quasi particle employ smaller $\beta_2$ values of ≈ 0.12 [Pop+79, Ric+77, Jer+94], while triaxial models have larger $\beta_2$ values of ≈ 0.20 → 0.23 [Kel+85, Kal+79]. The present neutron-scattering interpretations support the larger $\beta_2$ values of ≈ 0.20.

Total cross sections calculated with the SOM and ROTM are compared with energy averages of the measured values in Fig. 4.3.2. The results obtained with the two models are essentially identical (and the ROTM and VIBM results are very similar), thus decreasing $\beta_2$ from ≈ 0.2 has little effect on $\sigma_t$. Increasing $\beta_2$ to ≈ 0.25 results in a markedly "flatter" and less suitable energy distribution of the total cross section. Both the SOM and ROTM give results within several percent of the measured values from ≈ 1.5 → 7 MeV. At the upper energy limit of 10 MeV both are higher then the measured values by ≈ 8%, and both are slightly lower below ≈ 1.5 MeV. The energy-averaged measured total cross sections are probably known to ≈ ± 2 → 3%, and the normalization of the present scattering results at 10 MeV is

probably uncertain by ≈ 3 → 4%, so the discrepancy between measured and calculated total cross sections is, at most, just beyond the combined reasonable uncertainty in the two components, however the difference is systematic. Hopefully, the situation would be considerably improved if differential elastic-scattering data were available well above 10 MeV so as to better determine the energy dependencies of the models. Generally, global SOM's tend to give results 4 → 5% smaller than the average of the measured total cross sections at 10 MeV (e.g., refs. [BG69, Rap+79 and WG86]). The s- and p-wave strength functions calculated with the present models are compared with those deduced from experimental measurements in Table 4.3.2. All of the s-wave calculated values are larger than the experimentally deduced quantities, the most so for the SOM. This mass region is near the minimum of the s-wave strength function and SOM's typically over-predict the experimental values by rather large amounts (e.g., the models of refs. [BG69 and WG86]). The calculated p-wave strength functions are in better agreement with the experimental values, with differences that are only modestly beyond the experimental uncertainty alone. The present models include a spin-orbit term with the parameters taken from ref. [WG86]. That reference emphasizes polarization phenomena and thus the potentials should give appropriate polarization results. However, that can not be verified experimentally as scattered-neutron polarization data is very limited [Jon74].

The SOM, ROTM and VIBM real-potential strengths of the present work are similar, and are in reasonable agreement with the SOM of the preliminary report of ref. [SG82] based only on data at energies of less than 4 MeV. Generally, the real strengths of the collective potentials are slightly larger than that of the SOM (by 10 → 15 MeV-fm$^3$, or 3 → 4%) as has been generally been observed elsewhere [Smi95]. There are some spherical silver proton potentials found in the literature (13 are given in ref. [PP76]). These proton potentials are of variable quality but the real-potential strengths (in volume integrals per nucleon) are reasonably consistent and suggest a systematic strength of $J_v = 496.4 - 4.4213 \cdot E$ MeV-fm$^3$ when corrected for coulomb effects using the conventional formulation $V_c = 0.4 \cdot Z/A^{1/3}$. This proton $J_v$ should be related to the present SOM (Table 4.3.1) through the well known expression $J = J_o(1 \pm \xi \cdot \eta)$ [Lan62], where $\eta$ is the asymmetry $\eta = (N-Z)/A$, "+" ("-") is for protons (neutrons), and $\xi$ is a constant. The energy dependence of the $J_v$ derived from the proton potentials is approximately equivalent to that of the present SOM and the difference in magnitudes imply a value of $\xi \approx 0.4$, depending upon which energy is used in making the comparison. That value of $\xi$ is reasonably consistent with the predictions of the theory of nucleon-nucleon forces and other work [GPT68, GMP70] which

indicates $\xi \approx 0.45 \rightarrow 0.5$.

The present real potentials (Tables 4.3.1, 4.4.1 and 4.4.2), and the neutron potential implied by (p,p) studies, tend to have real strengths that are $\approx 10 \rightarrow 40$ MeV-fm$^3$ larger than given by global models (e.g., refs. [BG69, Rap+79, and WG86]) or by systematic studies of the mean potential field [Bau+82]. This is not surprising as the global potentials were deduced from considerations 10 MeV and more above the present scattering studies. This implies that dispersive contributions to the global potentials were small. These dispersive effects are given by the well known expression

$$J_v = J_{HF} + \frac{P}{\pi} \int_{-\infty}^{+\infty} \frac{J_{ws}(E')}{E - E'} dE', \qquad (1)$$

where $J_{HF}$ is the local-equivalent Hartree-Fock potential, $J_{ws}$ is the strength of the surface-imaginary potential, and P denotes the principle value of the integral [Sat83]. The limited energy scope of the neutron-scattering information and the complexity of the experimental resolution thwarts an effective dispersive interpretation of the present measurements. However, the integral of Eq. 1 can be estimated using one of the global models based upon higher-energy studies. Following that approach, the integral of Eq. 1 was evaluated using the global models of ref. [Rap+79] and ref. [BG69] and a fermi energy of -8.23 MeV. The results indicate that the present potentials, based upon neutron scattering at $\lesssim 10$ MeV, should have real strengths $\approx 20 \rightarrow 40$ MeV-fm$^3$ larger than an extrapolation of the global potentials to the same energy range. That difference is consistent with the larger real strengths of the present potentials, and with low-energy trends of neutron models implied by (p,p) studies. The $r_v$ of the present potentials are reasonably consistent with one another and tend toward the larger values frequently encountered in low-energy neutron studies. However, dispersive effects will lead to a decrease of $r_v$ with energy. The phenomena was not evident in the present cases, probably due to the limited energy range of the data base. The $a_v$ values of the present potentials are "conventional" with differences that probably only reflect minor variations in the fitting procedures. The present imaginary-potential strengths are similar, with strengths decreasing with energy up to $\approx 7$ MeV, with then a slow increase. Below $\approx 4$ MeV the SOM imaginary strength is larger than that of the ROTM or VIBM. The $r_w$ are quite large but, in the collective models, decrease with energy. All the imaginary strengths are approximately the same at $\approx 8 \rightarrow 10$ MeV. The $a_w$ increase with energy as has been widely observed at this laboratory and as is intuitively reasonable. Generally, the present potentials are applicable only to energies of $\lesssim 10$ MeV. Extrapolation to much

higher energies leads to peculiar behavior, particularly of the imaginary potential, and is not valid.

The above discussion gives emphasis to the SOM and ROTM. However, the ROTM and VIBR will give essentially the same quality description of the neutron processes. Thus, while the available information on neutron interaction with silver clearly indicates the importance of direct collective processes it does not differentiate between a vibrational and rotational interaction mechanism. Indeed, a successful study of proton scattering from $^{107}$Ag used a vibrational model in both DWBA and CCM interpretations [For+67], and a limited neutron study was reasonably successful assuming a vibrational interaction [Lag80]. On the other hand, some spectroscopic studies strongly suggest a rotational mechanism [Pop+79, Ric+77, Kel+85]. The present work does not resolve this dichotomy. The major limitation in the present work was the unavailability of reliable differential scattering data at energies well above 10 MeV, particularly on an isotopic basis.

Acknowledgments

The author is very much indebted to Dr. J. Raynal for the provision of the coupled-channels code ECIS95, and for instructions as to its use.

## References


[Bau+82] M. Bauer, H. Hernandez-Saldana, P.E. Hodgson and J. Quintanilla, J. Phys. G8 525 (1982).

[Bec+66] R. Becker, W. Guindon and G. Smith, Nucl. Phys. 89 154 (1966).

[BG69] F. D. Becchetti, Jr. and G. W. Greenlees, Phys. Rev. 182 1190 (1969).

[Buc+66] S. Buccino, C. Hollandsworth and P. Bevington, Z. Phys. 193 103 (1966).

[CB67] A. D. Carlson and H. H. Barschall, Phys. Rev. 158 1147 (1967).

[CL55] L. Cranberg and J. Levin, Proc. Conf. on Peaceful Uses of Atomic Energy, Geneva (United Nations Press, New York, 1955).

[CSL83] Nuclear Standards File, IAEA Tech. Report 227, eds. H. Conde, A. Smith and A. Lorenz (1983).

[Dro87] M. Drosg, IAEA Report, IAEA-TECDOC-410 (1987).

[FG71] D. Foster and D. Glasgow, Phys. Rev. C3 576 (1971).

[For+67] J. L. C. Ford Jr., Cheuk-Yin Wong, Taro Tamura, R. L. Robinson and P. H. Stelson, Phys. Rev. 158 1194 (1967).

[GC65] A. Gilbert and A. Cameron, Can. J. Phys. 43 1446 (1965).

[GMP70] G. W. Greenlees, W. Makofske and G. J. Pyle, Phys. Rev. C1 1145 (1970).

[GPT68] G. W. Greenlees, G. J. Pyle and Y. C. Tang, Phys. Rev. 171 1115 (1968).

[HF52] W. Hauser and H. Feshbach, Phys. Rev. 87 362 (1952).

[Hod71] P. E. Hodgson, Nuclear reactions and nuclear structure (Clarendon, Oxford, 1971).

[Jer+93] D. Jerrestam, S. Mitarai, E. Ideguchi, B. Fogelberg, A. Gizon, J. Gizon, W. Klamra, Th. Lindblad, R. Bark, J. Nyberg, M. Piiparinen and G. Slettin, Nucl. Phys. A557 411 (1993).

[Jer+94] D. Jerrestam, W. Klamra, J. Gizon, F. Liden, L. Hildingsson,J. Kownacki, Th. Lindblad, and J. Nyberg, Nucl. Phys. A577 786 [1994].

[Jer+94A] D. Jerrestam, W. Klamra, J.Gizon, B. Fogelberg, S. J. Freeman, H. J. Jensen, S. Mitarai, G. Sletten and I. Thorslund, Nucl. Phys. A579 256 (1994).

[Jon74] C. Jonker, Nucl. Phys A222 93 (1974).

[Kal+79] A. W. B. Kalshoven, H. H. A. Hesselink, T. J. Ketel, J. Ludziejewski, L. K. Peker, J. J. Van Ruyven and H. Verheul, Nucl. Phys. A315 334 (1979).

[Kel+85] H. J. Keller, S. Frauendorf, U. Hagemann, L. Kaubler, H. Prade and F. Stary, Nucl. Phys. A444 261 (1985).

[Lag80] Ch. Lagrange, Brookhaven National Laboratory Report, BNL-NCS-51363 (1980).

[Lan62] A. M. Lane, Nucl. Phys. 35 676 (1962); also Phys. Rev. Lett. 8 171 (1962).

[Mac+88] A. O. Macchiavelli, J. Burde, R. M. Diamond, C. W. Beausang, M. A. Deleplanque, J. J. McDonald, F. S. Stephens and J. E. Draper, Phys. Rev. C38 1088 (1988).

[MDH81] S. F. Mughabghab, M. Divadeenam and N. E. Holden, Neutron cross sections (Academic, New York, 1981).

[Mol80] P. A. Moldauer, Nucl. Phys. A344 185 (1980).

[Mol82] P. A. Moldauer, Spherical optical model code ABAREX, private communication (1982); modified by S. Chiba for elemental use.

[MS62] P. Malmberg and S. Snowdon, Phys. Rev. 128 351 (1962).

[MW66] J. Meadows and J. Whalen, Argonne National Laboratory Report, ANL-7210 (1966).

[NDS] Jean Blachot, Nucl. Data Sheets 41 111 (1984); B. Harmatz, Nucl. Data Sheets 34 643 (1981).

[Paa73] V. Paar, Nucl. Phys. A211 29 (1973).

[Pop+79] R. Popli, J. A. Grau, S. I. Popik, L. E. Samuelson, F. A. Rickey and P. C. Simms, Phys. Rev. C20 1350 (1979).

[PP76] C. M. Perey and F. G. Perey, At. Data and Nucl. Data Tables 17 1 (1976).

[PW83] W. P. Poenitz and J. F. Whalen, Argonne National Laboratory Report, ANL/NDM-80 (1983).

[Rap+79] J. Rapaport, V. Kulkarni and R. W. Finlay, Nucl. Phys. A330 15 (1979).

[Ray95] J. Raynal, private communication (1995); see also CEA Report, CEA-N-2772 (1994).

[Ric+77] F. A. Rickey, J. A. Grau, L. E. Samuelson and P. C. Simms, Phys. Rev. C14 1530 (1977).

[Rob+70] R. L. Robinson, F. K. McGowan, P. H. Stelson and W. T. Milner, Nucl. Phys. A150 225 (1970).

[Sat83] G. R. Satchler, Direct nuclear reactions (Clarendon, Oxford, 1983).

[SG82] A. B. Smith and P. T. Guenther, Argonne National Laboratory Report, ANL/NDM-66 (1982); see also Nucl. Phys. A415 1 (1984).

[SGM82] A. B. Smith, P. T. Guenther and R. D. McKnight, Proc. Conf. on Nucl. Data for Sci. and Technology, p. 39, ed. K. H. Boeckhoff (Reidel, Dordrecht, Holland, 1982).

[Smi+79] A. Smith, P. Guenther, G. Winkler and J. Whalen, Nucl. Phys. A332 297 (1979).

[Smi91] A. B. Smith, Argonne National Laboratory memorandum (1991), unpublished.

[Smi+92] A. B. Smith and P. T. Guenther, Argonne National Laboratory Report, ANL/NDM-127 (1992); S. Chiba, P. Guenther, A. Smith, M. Sugimoto and R. Lawson, Phys. Rev. C45 1260 (1992); C. Budtz-Jorgensen, P. Guenther, A. Smith and J. Whalen, Z. Phys. A306 265 (1982); A. Smith, P. Guenther, R. Larsen, C. Nelson, P. Walker and J. Whalen, Nucl. Instr. and Methods 50 277 (1977); and references cited therein.

[Smi95] A. B. Smith, Argonne National Laboratory Report, ANL/NDM-136 (1995); also see Nucl. Phys. A605 269 (1996).

[SR76] H. A. Smith and F. A. Rickey, Phys. Rev. C14 1946 (1974).

[VS65] W. Vonach and A. Smith, Nucl. Phys. 78 389 (1965).

[WG86] R. L. Walter and P. P. Guss, Proc. Conf. on Nucl. Data for Basic and Applied Sci., eds. P. Young et al., vol. 2, p. 277 (Gordon and Breach, New York, 1986).

[You86] For example see; P. G. Young, NEA Report, NEANDC-222U (1986).